Unpinning of scroll waves attached to multiple heterogeneities

Dhriti Mahanta and Sumana Dutta*
Department of Chemistry, Indian Institute of Technology Guwahati, Guwahati 781039, India

(Received 27 April 2018; published 7 November 2018)

Scroll waves in reaction diffusion systems can be pinned to several unexcitable heterogeneities. The stable pinned filaments have highly enhanced lifetimes. An external gradient can be applied to unpin the scroll waves sequentially from the anchoring sites. As the number of pinning sites are increased, the strength of the field required to unpin the filament also increases. The time required for unpinning changes as a function of the number of anchors, the geometry in which they are arranged, and their placement relative to the external field direction. Experiments with the Belousov-Zhabotinsky reaction are supported by numerical simulations on a simple reaction diffusion model.

DOI: 10.1103/PhysRevE.98.052206

I. INTRODUCTION

Spiral and scroll wave activities are often witnessed in nature. These are two- and three-dimensional excitation wave patterns, found in systems such as the *Dictyostellium discoideum* [1], neural cortex [2], retinal cells [3], and cardiac tissues [4]. Such structures are also observed in very diverse and unrelated environments, such as fluid flows [5], liquid crystals [6], and galactic formations [7]. A plane traveling wave may break-up and form a pair of spirals, when it encounters an unexcitable heterogeneity or an area of low excitability in its path of motion [8]. Depending on the size and geometry of the heterogeneity, the spiral may also get attached to it [9]. This phenomenon of pinning is also displayed by the three-dimensional scroll waves, when their one-dimensional filaments get anchored to obstacles of different kinds [10]. Free scroll waves can have either positive or negative filament tension, according to which they either shrink and collapse or keep on expanding till they reach the system boundary, in accordance with curvature-dependent motion [11]. As a result of pinning, the lifetime of the filaments are infinitely elongated. When this occurs in the cardiac tissues, the scroll waves responsible for disturbing the rhythm of the heart become long-lived and threaten the very existence of the individual [8]. Unpinning of the waves from the obstacles ensure that they can subsequently undergo free curvature-dependent dynamics. So, the study of the pinning and unpinning of spiral and scroll waves is also of importance to medical science, over and above its fundamental academic relevance.

Chemical systems, such as the Belousov-Zhabotinsky (BZ) reaction, are good candidates for the tabletop study of such processes. This is a system with positive filament tension, where the scroll wave filaments eventually collapse and disappear [12,13]. Scroll waves in the BZ have been shown to pin to spherical glass beads, cylinders, tori, and extended meshes [14–16]. Depending on the nature of the heterogeneity, the collapse of the filaments can be partially or completely stopped. The dynamics of spiral and scroll waves in the otherwise homogeneous reaction diffusion systems have been modified and controlled by employing external forces, like electric fields, concentration, and thermal gradients [17,18]. Free scroll waves drift under the influence of such fields, and their orientation is modified, depending on their position relative to the field direction. Dynamic and cross electric fields and thermal gradients have made the scroll waves trace cyclic trajectories [19]. In studies of pinned filaments, it has been demonstrated that scroll waves pinned to two spherical beads can be unpinned by the application of such gradients [20,21]. However, it has been inferred from some recent work on the BZ system that as the anchor size changes, the rigidity of the filament also gets modified [22]. The number of pinning sites and the geometry in which they are arranged could also be factors influencing the stability and dynamics of the pinned filament. In this work, we carry out experiments in the homogeneous BZ system, to study the pinning of the scroll waves to multiple spherical heterogeneities, placed in different geometries. We then try to unpin them from their stably pinned configurations, using steady electric fields and thermal gradients. The influence that the bead size and bead placement has on the phenomenon of unpinning has been studied in detail. An interesting trend is found in the unpinning time as the number of pins increases. The study is complemented by numerical simulations based on the Barkley model for reaction-diffusion systems.

II. EXPERIMENTAL METHODS

We used the three-dimensional, Ferroin-catalyzed BZ reaction for our experiments. Spherical glass beads were employed to act as the heterogeneous obstacles. The reactions were performed in a specially designed reaction chamber (8 cm × 8 cm × 2.5 cm) having heat exchangers on its two sides that were connected to thermostat-controlled water baths. All reactions were carried out at room temperature. The experimental system consisted of two layers of BZ containing 0.8 wt/vol% agarose gel. Each layer was about 4 mm thick, and the initial concentrations of the reactants used were

*sumana@iitg.ac.in

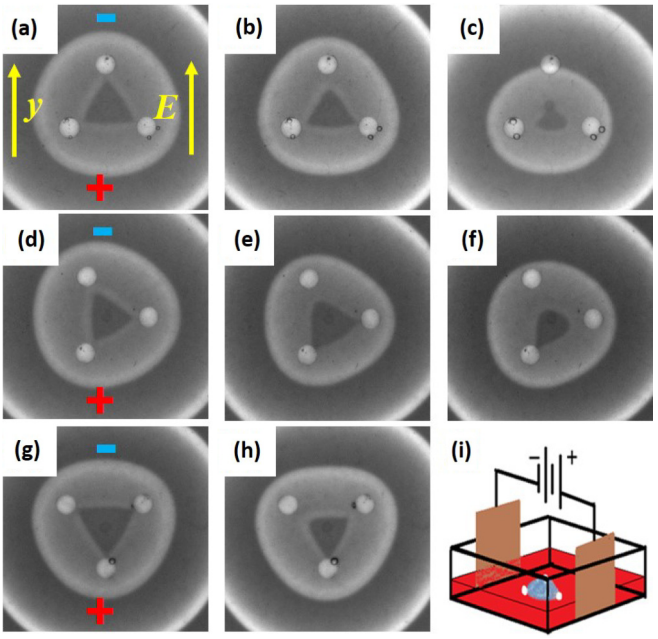

FIG. 1. Sequential unpinning of scroll waves from three beads in the presence of an external electric field gradient of strength 0.25 V cm^{-1}. An area of 1.91 cm × 1.91 cm is covered in each snapshot. The bright circles are obstacles of diameter 1.8 mm separated by a distance of 7.3 mm from one another. Panels (a, d, g) are snapshots of stabilized scroll waves before the application of the electric field. The position of the anode and cathode are being designated by "+" and "−" in each experiment. Time lapsed after the application of the electric field is (b) 16.6 min and (c) 45 min in the first experiment; (e) 20 min and (f) 28 min in the second experiment; and (h) 35.6 min in the third experiment. (i) Schematic diagram of an experiment with bead positions as in (g). Movies available in the Supplemental Material [13].

$[NaBrO_3] = 0.04$ M, $[CH_2(COOH)_2] = 0.04$ M, $[H_2SO_4] = 0.16$ M, and $[Fe(o\text{-}phen)_3]SO_4 = 0.5$ mM. All solutions were prepared using Millipore water. The first layer of BZ was poured into the reaction chamber, and the required number of glass beads were embedded halfway into the forming gel. Once the gelation process was complete, the tip of a clean silver wire was slightly inserted into the gel for a few seconds, at a position equidistant from the glass beads. This initiated the formation of a chemical wave, by the local removal of the inhibitory Br^- ion, in the form of AgBr. When the expanding wave reached the glass beads, the second BZ gel layer, slightly above its gelling temperature, was poured over the system. The semispherical wave in the lower gel layer immediately started to curl up into the top layer and eventually formed the scroll ring of desired dimension. For the application of electric fields, two rectangular Cu electrodes (sized 2.5 cm × 3.5 cm) were vertically placed along the walls, perpendicular to the heat exchangers such that the scroll was equidistant from the Cu plates [Fig. 1(i)]. The electrodes were connected to a DC power supply (Scientific Multipurpose Power Supply PSD3304). The heat exchangers along the reaction chamber could act as temperature stabilizers to compensate for Ohmic heating. Alternatively, they could also be used for introducing thermal gradients into the system. The experiments were recorded as sequential snapshots with a charge coupled device (CCD) camera mounted above the reaction chamber, which was illuminated with a cold, diffused white light source from below. A blue dichroic filter was fitted to the camera to facilitate contrast enhancement. The images were recorded onto a computer which were later analyzed using MATLAB codes.

III. EXPERIMENTAL RESULTS

It is known that a free scroll ring in the BZ system has a positive filament tension, i.e., it shrinks with time, and finally disappears [12]. When it is attached to heterogeneous obstacles, the pinning of the wave stops the shrinkage, and stabilizes the size of the wave. In the presence of electrical and thermal gradients, scroll waves pinned to two beads were successfully unpinned and eventually removed from the system [20,21]. In this paper, we look at scenarios where the scroll waves are pinned to three, four, or six glass beads. We carried out several experiments with different geometries for a fixed number of pinning sites, and we observed that the pinning was strongest for the regular geometries, i.e., equilateral triangle for three pinning sites, square for four pinning sites, and hexagon for six pinning sites. Here, stronger pinning means it is a stabler configuration and requires more time to unpin, as compared to the other geometries. For example, a scroll pinned to three beads arranged as an isosceles triangle will unpin much faster than one that is pinned to the beads placed at vortices of an equilateral triangle. Even in the absence of any field, the pinning may not be stable for some scalene triangular geometries, and the scroll might unpin spontaneously from one or more beads. This could be because of the competition between filament tension and rigidity [22]. For our unpinning experiments, we report only the examples with regular geometries.

Figure 1 shows three experiments where an electric field was applied to unpin the scroll waves attached to three beads, which were arranged in the form of an equilateral triangle. In each of these experiments, the relative position of the electric field with respect to the triangle was varied. Sequential snapshots of the experiments are shown in Fig. 1. In the first snapshot of each experiment [Figs. 1(a), 1(d), 1(g)], a bright, narrow band is seen attached to the three beads, in the form of a triangle. This is the initial position of the filament, which emits inward and outward propagating waves. The waves that propagate inward collide shortly after emission, and disappear (can be observed in the movies in the Supplemental Material [13]). The outward propagating waves, however, are seen as bright bands on the dark background. The small black circles that seem to grow with time, are CO_2 bubbles, which are a product of the reaction. Once the scroll ring was stably pinned to the beads (after more than one hour of scroll wave initiation), an electric field was applied along the positive y-direction. In the first experiment [Figs. 1(a)–1(c)], the anode lay near the base of the triangle, so that the two basal beads were equidistant from the anode. The scroll ring first unpinned from the bead nearest to the cathode [Fig. 1(b)], and then simultaneously from the two basal beads [Fig. 1(c)]. In the second experiment [Figs. 1(d)–1(f)], the beads were placed so that the altitude of the formed triangle was at right angles to

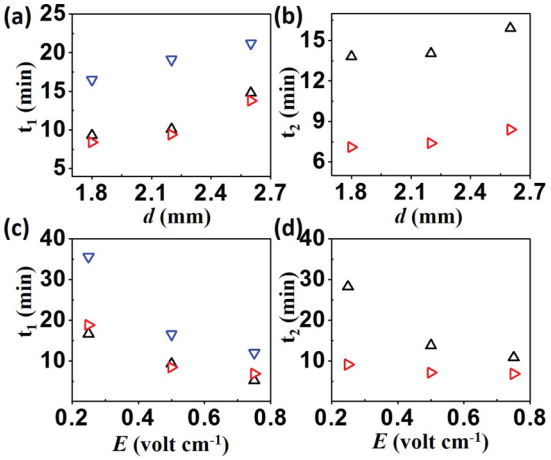

FIG. 2. Dependence of unpinning time t_1 and t_2 on (a, b) bead diameter and (c, d) electric field strength. The electric field strength has been maintained at 0.5 V cm^{-1} for all experiments in (a) and (b) and the bead diameters are 1.8 mm in (c) and (d). Black triangles, red tilted triangles and blue inverted triangles are used for three different orientations corresponding to Figs. 1(a), 1(d), and 1(g), respectively.

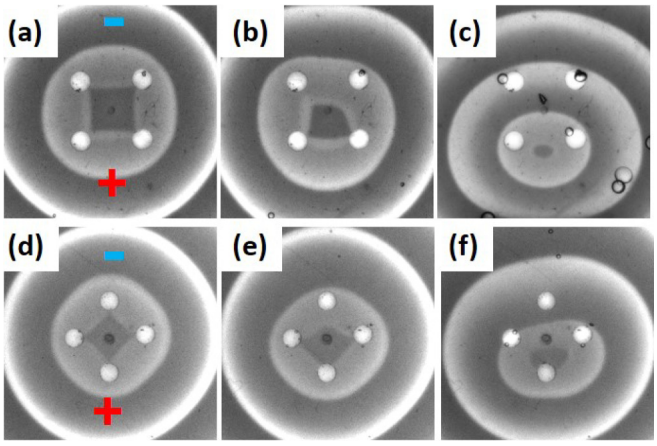

FIG. 3. Unpinning of scroll waves pinned to four beads. Panels (a, d) are snapshots of stabilized scroll waves in the absence of an external field. Time-lapse after application of electric field in subsequent images in the first experiment are: (b) 21.6 min and (c) 93.6 min, respectively. In the second experiment, they are (e) 7 min and (f) 20 min, respectively. Direction of the external field is along the y axis (from "+" to "−") in both experiments, and the electric field strength is 0.5 V cm^{-1}. The bead size and the separation between the nearest beads are 2.26 mm and 6.5 mm, respectively, for the first experiment; while for the second, they are 2.0 mm and 5.4 mm, respectively. An area of 2.26 cm × 2.26 cm is covered in each snapshot. Movies available in the Supplemental Material [13].

the electric field direction. In this scenario, the three beads were at different distances from the electrodes. The result was that the scroll unpinned first from the bead closest to the cathode, followed by the second bead, and finally it disappeared at the third bead which was nearest the anode. Finally, when the base of the triangle was nearer to the cathode [Fig. 1(g)], the application of electric field made the scroll unpin from the two basal beads simultaneously [Fig. 1(h)]. The scroll wave eventually shrunk and remained attached to the third bead till the end.

It has been inferred from earlier studies [14] that the size of the obstacles change the nature of the filament pinned to it. We wanted to see if there was any effect of the size of the pinning beads to the unpinning of the filament, under the influence of electric field. We carried out three sets of experiment for each of the bead orientations (as shown in Fig. 1), and plotted the time required for the first and second unpinning of the scroll as a function of bead diameter. Figures 2(a) and 2(b) show the variation in the unpinning times t_1 and t_2, respectively. It is observed that the unpinning time increases with the increase in the bead diameter. For the first unpinning, the time required in the case where the scroll unpins simultaneously from two beads [like the experiment in Fig. 1(g)], is much higher than in the other two cases. For the latter two orientations, t_1s are similar, with a slightly larger value when the beads are placed as in Fig. 1(a). However, when we consider the second unpinning time t_2, we realize that there is no t_2 for the layout of the beads as shown in Fig. 1(g). In the other two orientations, the time required for the scroll to unpin from two beads simultaneously [like in Fig. 1(a)] is much larger than where it unpins from only one [Fig. 1(d)]. Also, interestingly, the variation in t_2 is much less as compared to t_1, with increasing bead size.

To study the effect the strength of the electric field has on the unpinning of the scroll wave, we carried out several experiments, where we varied the electric field strength, while keeping the bead diameter constant. Figures 2(c) and 2(d) summarize the results of nine experiments, with three different values of the field strength. It was seen that the unpinning time reduced as the electric field strength was increased, for all the different orientations of the three obstacles. As in the case of varying bead diameter, in these experiments too, unpinning time is much higher when the scroll has to detach simultaneously from two beads. There is almost no visible difference in t_1 for the other two orientations. Similar observation was made for t_2.

Next, we carried out experiments with four beads. Figure 3 shows snapshots of two such experiments, where the bead size and electric field strengths are kept constant. In the two examples, only the orientation of the beads, with respect to the electric field direction was changed. In the first experiment [Figs. 3(a)–3(c)], the beads are placed in a manner, such that there are two sets of beads, equidistant from the cathode. So, the scroll consecutively unpins from two beads at a time. This results in high unpinning times. In the second experiment [Figs. 3(d)–3(f)], the first unpinning is from a single bead, and that takes comparatively much shorter time. While the second unpinning occurs simultaneously from two beads, this requires a much larger time. This time of ∼20 min is also comparable to the time required for the first unpinning in the prior experiment [Fig. 3(b)]. In the case of the three-bead-pinning experiments, contrarily, such comparison between simultaneous two-bead unpinnings show that t_2 is always smaller than t_1. As for example, 14 versus 16 min for $d = 1.8$ mm, $E = 0.5$ V cm^{-1}; 16 versus 22 min for $d = 2.6$ mm, $E = 0.5$ V cm^{-1}; 28 versus 35 min for $d = 1.8$ mm, $E = 0.25$ V cm^{-1}; etc. [Fig. 2]. This suggests

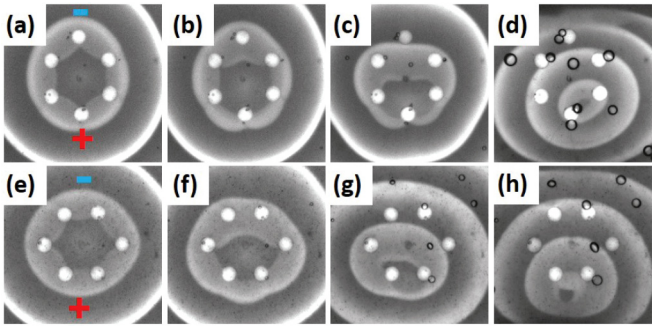

FIG. 4. Electric field unpinning of scroll waves attached to six beads. (a, e) are snapshots of stabilized scroll waves before the application of the field. In the first experiment, (b) 5.2 min, (c) 24.7 min, and (d) 130.7 min have passed after the onset of electric field. While in the second experiment, the panels have been chosen after (f) 12.5 min, (g) 40.3 min, and (h) 98 min have passed. The electric field strength is 1.0 V cm^{-1}, the bead size is 2.26 mm, and the smallest inter-bead distance is ∼5.1 mm, in both these experiments. An area of 2.26 cm × 2.26 cm is covered in each snapshot. The electrode positions are shown by the "+" and "−" symbols in (a) and (e). Movies available in the Supplemental Material [13].

that there is an essential difference in the filament shape, when it is pinned to three obstacles as compared to four obstacles. Also, as we increase the number of beads from three to four, the electric field required for successful unpinning increases. Experiments were also carried out for scroll rings pinned to six beads arranged in the form of a hexagon. With more beads, these experiments became much more complicated. There were two main challenges; one was the short time window available to place the beads, before the gelation of the first layer. This resulted in a not-so-perfect hexagonal placement of the beads. The other was that higher strengths of the electric field was required to unpin the scroll wave that was attached to six beads. This resulted in huge expansions of the scroll wave, which eventually touched the reaction chamber when it started rotating on its symmetry axis, and resulted in ring breakage. Experiments for scroll rings attached to two hexagonal orientations of six beads each, are shown in Fig. 4. We have successfully been able to unpin the scroll waves from their six-point anchors, using moderately high electric fields. The trends in the unpinning times are similar to the previous experiments.

Similar experiments were carried out for studying the unpinning of scroll waves attached to multiple obstacles, under the influence of a thermal gradient [13]. For low and moderate strengths of thermal gradients, the pinned scroll waves were successfully unpinned, and eventually shrunk and disappeared. However, for comparatively higher strengths of thermal gradient, the waves were seen to expand in size, and remained pinned to the obstacles. Unlike in the case of electric field, here we were not successful in observing any exact trend in the unpinning times, with gradient strength.

IV. NUMERICAL SIMULATIONS

To gain a better insight into the filament dynamics, as the scrolls unpin under the influence of the external gradients, we carried out numerical simulations of the three-dimensional Barkley model [23]. This is a two-variable activator-inhibitor model, which has been widely used to study pattern forming systems like the BZ reaction and other reaction-diffusion systems [12,15,16,22,24]. In the presence of an external flux, the two coupled nonlinear differential equations take the following form [19–21]:

$$\frac{\partial u}{\partial t} = \frac{1}{\epsilon}\left\{u(1-u)\left(u - \frac{v+b}{a}\right)\right\} - \nabla J_u,$$
$$\frac{\partial v}{\partial t} = u - v - \nabla J_v.$$

In the presence of diffusion alone, $J_u = -D_u \nabla u$, and $J_v = -D_v \nabla v$, where $D_u = 1.0$ and $D_v = 1.0$, are the diffusion coefficients. When an electric field is applied to the system, the fluxes modify as: $J_u = -D_u \nabla u + D_u z_u u E$, and $J_v = -D_v \nabla v + D_v z_v v E$, where E is the strength of the applied electric field, and z_u and z_v are the charges on u and v, respectively [19]. The variables in the Barkley model, u and v, are loosely related to the concentrations of the bromous acid and the oxidized form of the indicator, ferroin, respectively. So, we consider $z_u = 0.0$ and $z_v = 3.0$. The values of the system parameters were chosen as $a = 0.84$, $b = 0.07$, and $\epsilon = 0.02$. Under these conditions the filament of the scroll wave showed zero drift along the binormal direction.

The reaction system was modeled as a three-dimensional lattice measuring $160 \times 160 \times 160$ grid points having zero flux boundaries for all diffusing species along the external boundaries. The obstacles were defined as spherical regions where the value of the variables u and v are zero. Neumann boundary conditions around these obstacles also yield identical results. The two partial differential equations were numerically integrated using explicit Euler integration scheme and a nineteen point Laplacian stencil with an integration time step of 0.012 and grid spacing of 0.35. The filament of the scroll is identified at regions having $u = 0.5$ and $v = a/2 - b$. The scroll wave is initiated similar to the experiment, by allowing a semispherical wave in the bottom half of the system, to curl up into the top half. The scroll is made large enough, so that its circular filament encompasses the geometry traced by the multiple obstacles. Over time, the filament shrinks and the scroll wave attaches to the obstacles. Once, it is stabilized around the obstacles, and shrinking ceases, the electric field is subsequently introduced numerically into the system.

For simulations which employ external thermal gradient, the flux of the species u (for v replace u by v) is given by, $J_u = -D_u \nabla u - D_{T_u} u(1-r_u)\nabla T$ [25]. Here, $D_{T_u} = D_u S_{T_0}/(1 + k_s u)$ is the thermal diffusion coefficient of u where $S_{T_0} = -0.1$, is the Soret coefficient and $k_s = 1.0$, is a phenomenological constant. $r_u = u/c_T$, is the relative concentration of u, where $c_T = u + v$, and ∇T is the thermal gradient along the y direction. The negative value of the Soret coefficient indicates the movement of the particles toward the hot end of the reaction chamber. The flux for v is similarly modified, with identical values of S_{T_0} and k_s.

We carried out numerical simulations for unpinning of scroll waves attached to multiple beads (two to six), arranged in regular geometries. The wave nature and filament dynamics of one such simulation is depicted in Fig. 5. This particular

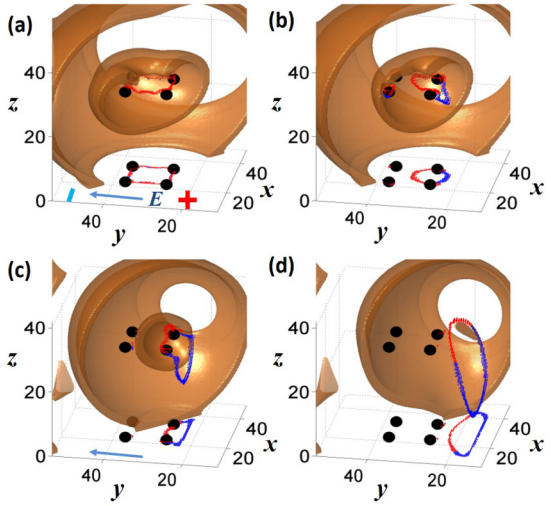

FIG. 5. Wave and filament dynamics of unpinning in the Barkley model. (a–d) The time evolution of the scroll wave (solid brown areas) and its filament (curves) which is initially pinned to four obstacles. The spherical obstacles (of diameter 2.8 space units, placed 10.5 space units apart) are designated as black balls. The sections of the filament above the plane containing the obstacles are indicated in red, while those below the plane, are drawn in blue. The curves along with the circles at the bottom of the box are the two-dimensional projections of the filament and the obstacles. Panel (a) shows the system before the application of electric field, $E = 0.05$ units. The time intervals between neighboring frames are 40.3, 34.1, and 40.8 time units, respectively. The computed volume has been cropped along the boundaries.

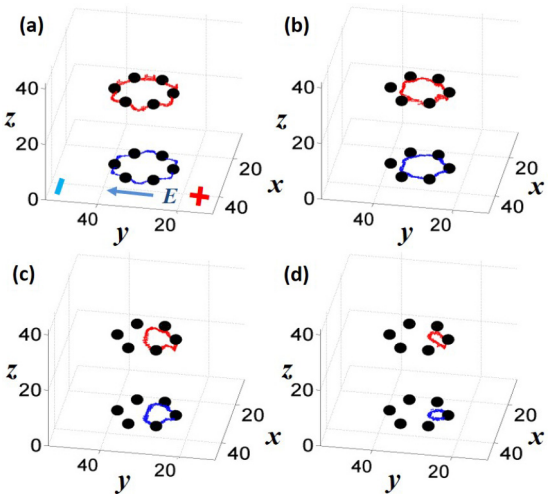

FIG. 6. Unpinning of a scroll wave attached to six obstacles arranged hexagonally. The (red) curves are the filaments, and the (black) spheres are the obstacles (of diameter 2.1 space units, placed 7.2 space units apart). The two-dimensional projections of the filaments are shown at the bottom of the box ($z = 0$). The electric field ($E = 0.05$ units) is applied in the y direction. (a) Stable filament attached to the six beads, before the application of electric field. (b–d) Sequential unpinning of the filament from the six beads. 22.6, 25.5, and 20.2 time units, respectively, have elapsed between neighboring frames. The computed volume has been cropped along the boundaries.

case is similar to the experiment illustrated in Figs. 3(a)–3(c). The solid brown waves are the regions where the system is excited, or $v > 0.4$. For the purposes of better visualization, only the rear half of the wave form is shown. In Fig. 5(a), the semispherical wave in the lower half of the cube is curling into the top half, while the filament is attached to all the four beads. The electric field is applied at this stage, in the direction of the y axis. The filament starts flipping perpendicular to this direction, as is seen from the separation of the same into red and blue portions. Subsequently, the filament detaches from the two beads further away from the anode [Fig. 5(b)]. Since these beads are equidistant from, and nearest to the cathode, the scroll detaches from them simultaneously. The scroll ring keeps on reorienting, as it moves in the direction opposite to the electric field [Fig. 5(c)]. Finally, it unpins from the remaining two beads [Fig. 5(d)], and becomes almost parallel to the z axis. After this, if the electric field is turned off, the free scroll wave will shrink due to its positive filament tension and disappear. The only difference between this simulation and the experiment in Figs. 3(a)–3(c), is that, in the latter case there is no visible expansion of the waves after it has detached from all the beads. In the case of the simulation, the field strength can be reduced to achieve complete unpinning of the vortex, while avoiding any expansion of the filament. As is evident from the experiments, the bead size and interbead distance will also play an important role in this.

Figure 6 shows the results of simulation for the experimental case depicted in Figs. 4(e)–4(h). We show only the filament dynamics in this case. Similar to the experiments, the filament detaches first from the bead furthest from the anode, i.e., the lone bead lying towards the extreme left along the y axis. Then it unpins simultaneously from the next two beads, which are equidistant from the anode [Fig. 6(b)]. At this stage, a slight flipping of the ring in the z direction is visible. The filament then detaches from the next two beads and shrinks in the vicinity of the last bead, in the extreme right along the y axis, which is nearest the anode [Fig. 6(d)]. The results for the other orientation of six beads can be found in the Supplemental Material [13].

We also carried out simulations for the case where four beads are placed identical to the experiment in Fig. 3(d). The simulations exactly mimicked the experiments. The results of the simulations for a scroll wave pinned to two, three, and five beads, also yielded expected results.

V. DISCUSSIONS AND CONCLUSIONS

With our experiments and numerical simulations, we have shown that scroll rings can be stably pinned to multiple heterogeneities. Such pinned vortices can also be sequentially unpinned by the application of controlled external gradients. Electric field and thermal gradients have been used in our experiments for this purpose. Scroll waves pinned at three to six sites were successfully unpinned by these methods. The experiments with electric fields can be more easily controlled, and hence give better results, and show several interesting trends. As we increased the number of pinning sites, we had to apply stronger electric fields for the successful unpinning of the waves. This also suggests that more the number of pinning

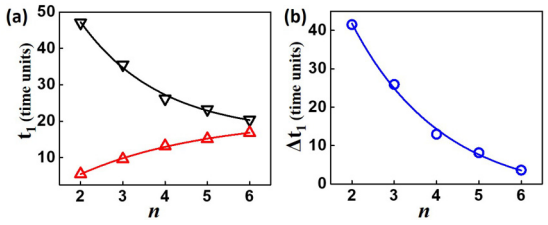

FIG. 7. Variation of unpinning time, with number of beads. (a) First unpinning time, t_1, as a function of the number of beads, n. The (black) upturned triangles are for the orientations, where the scroll unpins from two beads simultaneously [e.g., Figs. 1(g), 3(a), and 4(e)]. The (red) triangles are for the orientations, where the filament initially detaches from only one bead [e.g., Figs. 1(a), 3(d), and 4(a)]. (b) The difference between the first unpinning times, Δt_1, for the two different orientations in panel (a), as a function of n. The diameter of the obstacles are 3.5 space units in each case, and they are placed 10.5 space units apart. The applied electric field strength is 0.075 units.

sites, greater is the stability of the pinned structure. However, the relationship is not so simple, as it also depends on the size of the scroll wave, and hence the tension and rigidity of the filament sections between neighboring beads.

One very interesting observation could be made on the unpinning times of the scroll wave filament from different number of beads. Figure 7 illustrates this trend in the results of the numerical simulations. The first unpinning time, t_1, decreases rapidly as the number of beads increase, for those orientations where the scroll detaches from two beads simultaneously [Fig. 7(a)]. While the nature of change is opposite when it detaches from a single bead at first. The difference in these two unpinning values, Δt_1, is again a decreasing function of the number of beads [Fig. 7(b)]. The drop in Δt_1 values with increasing n could be due to the change in the final geometry of the pinned filament. A closed filament stably pinned to n beads could be thought of as consisting of n filament sections. For a regular geometry of beads, the arclength of these n filament sections are equal. As we change the orientation of a pinned filament with respect to the gradient, the time required for the first unpinning changes. When the filament unpins from two beads simultaneously, the time taken is appreciably more than that which is required to unpin from only one bead. However, as the number of pins increases, the gap between these two times decreases. When the number of obstacles is small, the difference is most evident. For example, when $n = 2$, unpinning from two beads simultaneously would mean unpinning of the entire scroll wave filament. On the other hand, while unpinning from one bead, the filament is still pinned at half the initial number of pins. As n becomes large, the filament is anchored at many points even after it has unpinned from one or two beads. For $n = 4$, the filament is pinned at two beads in the first scenario, as compared to three in the second (Fig. 3). And when $n = 6$, the ratio of pins is 4:5 after the first unpinning (Fig. 4). As the number of beads increases, the shape of the filament after the first unpinning from just one pinning site, differs progressively less from the case when unpinning occurs from two sites simultaneously. As a result, the term Δt_1 falls off with increase in the value of n. No such definite tendency could be extracted from the results of the experiments, because the electric field strength had to be increased as we increase the number of beads. Hence, we do not have enough data to get an exact comparison of t_1 with n (for a constant value of E). Nevertheless, the qualitative plot generated from the available experimental results show a similar trend in the values of t_1 and Δt_1 [13].

Future experiments could be designed to study the unpinning of scroll waves anchored to differently shaped heterogeneities, like rods, disks, and rings. Again, short electric pulses could be used for unpinning instead of using a continuous electric field. This may help alienate the expansion of the filament under the influence of strong electric fields. Other interesting variations could be changing the nature of the obstacles, like excitability and branching. Such modifications will shed more light on the dynamics of filaments occurring in natural systems, like cardiac tissues.

ACKNOWLEDGMENTS

This work was financially supported by the Science and Engineering Research Board, Government of India (Grant No. SB/S1/PC-19/2012).

[1] F. Seigert and C. J. Weijer, Proc. Natl. Acad. Sci. USA **89**, 6433 (1992).
[2] S. J. Schiff, X. Y. Huang, and J. Y. Wu, Phys. Rev. Lett. **98**, 178102 (2007).
[3] N. A. Gorelova and J. Bures, J. Neurobiol. **14**, 353 (1983).
[4] J. M. Davidenko, A. M. Pertsov, R. Salomonsz, W. Baxter, and J. Jalife, Nature (London) **355**, 349 (1992).
[5] P. Wiegmann and A. G. Abanov, Phys. Rev. Lett. **113**, 034501 (2014).
[6] I. Chuang, R. Durrer, N. Turok, and B. Yurke, Science **251**, 1336 (1991).
[7] A. Kamada, M. Kaplinghat, A. B. Pace, and H.-B. Yu, Phys. Rev. Lett. **119**, 111102 (2017).
[8] J. Jalife, M. Delmar, J. Anumonwo, O. Berenfeld, and J. Kalifa, *Basic Cardiac Electrophysiology for the Clinician*, 2nd ed. (Wiley-Blackwell, Oxford, UK, 2009).
[9] S. Nettesheim, A. von Oertzen, H. H. Rotermund, and G. Ertl, J. Chem. Phys. **98**, 9977 (1993).
[10] A. M. Pertsov, E. A. Ermakova, and A. V. Panfilov, Physica D **14**, 117 (1984).
[11] J. P. Keener and J. J. Tyson, SIAM Rev. **34**, 1 (1992).
[12] I. R. Epstein and J. A. Pojman, *An Introduction to Nonlinear Chemical Dynamics* (Oxford University Press, Oxford 1998).
[13] See Supplemental Material at http://link.aps.org/supplemental/10.1103/PhysRevE.98.052206 for movies of experiments and additional experimental and numerical data.

[14] Z. A. Jiménez and O. Steinbock, Phys. Rev. Lett. **109**, 098301 (2012).
[15] S. Dutta and O. Steinbock, J. Phys. Chem. Lett. **2**, 945 (2011).
[16] D. Mahanta, S. Dutta, and O. Steinbock, Phys. Rev. E **95**, 032204 (2017).
[17] C. Luengviriya, S. C. Müller, and M. J. B. Hauser, Phys. Rev. E **77**, 015201(R) (2008).
[18] M. Vinson, S. Mironov, S. Mulvey, and A. Pertsov, Nature (London) **386**, 477 (1997).
[19] N. P. Das and S. Dutta, Phys. Rev. E **96**, 022206 (2017).
[20] N. P. Das, D. Mahanta, and S. Dutta, Phys. Rev. E **90**, 022916 (2014).
[21] Z. A. Jiménez, Z. Zhang, and O. Steinbock, Phys. Rev. E **88**, 052918 (2013).
[22] E. Nakouzi, Z. A. Jiménez, V. N. Biktashev, and O. Steinbock, Phys. Rev. E **89**, 042902 (2014).
[23] D. Barkley, Physica D **49**, 61 (1991).
[24] A. T. Winfree, R. Kapral, and K. Showalter, *Chemical Waves and Patterns* (Springer, Netherlands, 1995).
[25] S. Dutta and D. S. Ray, Phys. Rev. E **75**, 066206 (2007).